TECHNOLOGY DEVELOPMENT FOR IRON FISCHER-TROPSCH CATALYSIS

Contract No. DE-AC22-91PC94055

Quarterly Technical Progress Report No. 5

Covering the Period October 1, 1995 to December 31, 1995

Prepared for

U.S. Department of Energy
Pittsburgh Energy Technology Center
PETC Project manager: Richard E. Tischer
P. O. Box 10940
Pittsburgh, PA 15236-0940

Submitted by

Project Manager: Burtron H. Davis
University of Kentucky Research Foundation
Kinkead Hall
Lexington, KY 40506-0057

Date Prepared
January 19, 1996

MASTER

2. Contract Objectives

The objective of this research project is to develop the technology for the production of physically robust iron-based Fischer-Tropsch catalysts that have suitable activity, selectivity and stability to be used in the slurry phase synthesis reactor development. The catalysts that are developed shall be suitable for testing in the Advanced Fuels Development Facility at LaPorte, Texas, to produce either low- or high-alpha product distributions. Previous work by the offeror has produced a catalyst formulation that is 1.5 times as active as the "standard-catalyst" developed by German workers for slurry phase synthesis. The proposed work will optimize the catalyst composition and pretreatment operation for this low-alpha catalyst. In parallel, work will be conducted to design a high-alpha iron catalyst this is suitable for slurry phase synthesis. Studies will be conducted to define the chemical phases present at various stages of the pretreatment and synthesis stages and to define the course of these changes. The oxidation/reduction cycles that are anticipated to occur in large, commercial reactors will be studied at the laboratory scale. Catalyst performance will be determined for catalysts synthesized in this program for activity, selectivity and aging characteristics.

The research is divided into four major topical areas: (a) catalyst preparation and characterization, (b) product characterization, (c) reactor operations, and (d) data assessment.

To accomplish the objectives of the project, these topics have been organized into the following technical tasks:

a. Task 1.0   Development of Optimum Promoter Levels for Low- and High-Alpha

               Catalysts

1.1 Determine Optimized Synthesis Procedure for High-Alpha Iron-Based Fischer-Tropsch Catalysts

- Role of precursor particle size on activity.

- Role of Cu in precipitated catalysts.

- Define attrition resistance.

1.2 Prepare Catalysts that can be Used to Determine the Role of Promoters for Low- and High-Alpha Catalysts

- Define optimum SiO_2.

- Define optimum Al_2O_3.

1.3 Prepare Catalysts that can be Used to Quantify the Role of K on Product Selectivity in both Low- and High-Alpha Catalysts.

1.4 Complete the Optimization of the Two Best Low-Alpha, Iron-Based Fischer-Tropsch Catalysts Developed during the Previous Contract.

b. Task 2.0 Definition of Preferred Pretreatment for both Low- and High-Alpha Fischer-Tropsch Catalysts.

2.1 Determine the Role of Cu in the Activation of Precipitated Low- and High-Alpha, Iron-Based Fischer-Tropsch Catalysts.

2.2 Determine the Effect of K Content on Activation Procedures and Determine if the Method of Addition has any Effect on Catalyst Activity and Life.

2.3 Determine the Physical and Chemical Changes that Occur during Catalyst Pretreatment and Use and Determine how these Changes Effect the Strength of the Catalysts.

3

2.4 Evaluate the Effect of Carbon Deposition during Catalyst Activation on Activity, Selectivity and Aging Characteristics.

c. Task 3.0 Catalyst Structure and Characterization.

d. Task 4.0 Catalyst Testing.

4.1 Verify the Quality of Data Obtained from the CSTR's.

4.2 Measure Catalyst Performance.

4.3 Determine the Stable Phases that Exist during Synthesis at Low and High CO Conversion Levels.

4.4 Obtain Data on the Rates Involved in the Interconversion of Iron Oxide and Iron Carbide.

e. Task 5.0 Reports.

3. Summary of Activities

Results have shown that promotion with copper greatly improves catalyst performance at 230°C for catalysts pretreated with carbon monoxide, hydrogen or syngas. Promising findings have been obtained for a 100Fe/4.4Si/2.6Cu/5.2K catalyst. Activation with syngas (H_2:CO=0.7) has been found to result in a more active catalyst than pretreatment with carbon monoxide or hydrogen when operating at low temperature. Syngas activation resulted in a carbon monoxide conversion greater than 65% at 230°C, 1.3 MPa, and space velocity (H_2:CO=0.7) of 3.1 NL h^{-1} g(Fe)$^{-1}$. Methane selectivity below 2.5 weight percent and C_{12}+ selectivity greater than 70% have been achieved. Total olefin selectivity for the C_2-C_{11} fraction was greater than 75% and was predominantly α-olefins.

Additional FTS runs are being made to optimize copper promotion and to determine how it affects FT activity. Early indications are that copper does increase

4

the rate of reduction in hydrogen of iron oxide to the zero valent state. As an example, activation of a 100Fe/3.6Si/0.71K catalyst with syngas at high pressure resulted in poor activity. Addition of copper to the catalyst resulted in a substantial increase in the carbon monoxide conversion from less than 15% to greater than 50%. X-ray diffraction and Mössbauer spectroscopy analyses show that without copper the catalyst was 100% Fe_3O_4; however, with copper the catalyst was composed of a mixture of Fe_3O_4 and iron carbides that are essential for high FT activity. Additional characterization is being conducted to determine the impact of copper on hydrogen and carbon monoxide treated catalysts.

4. Status, Accomplishments, Results and Discussion

A.0. - Task 1.0. Development of Optimum Promoter Levels for Low- and High-Alpha Catalysts

The goal of this task is to identify and optimize procedure for the preparation of iron-based catalysts that combine high activity selectivity and life with physical robustness. Each of the subtasks address an area of considerable uncertainty in the synthesis of catalysts.

A.1. Determine Optimized Synthesis Procedure for High-Alpha Iron-Based Catalysts

- Role of precursor size on activity.

  An Fe alumina supported catalyst was prepared in an attempt to make a robust catalyst with sufficient activity. The catalyst was prepared by impregnating alumina with 15 wt.% Fe, followed by a reduction and passivating step. A second impregnation of 15 wt.% Fe (30 wt.% Fe total) was added to this preparation and the reduction and passivating

5

step repeated. The catalyst was tested in the CSTR. CO conversions of approximately 50% were obtained. This is encouraging activity for this first preparation.

- Role of Cu in precipitated catalysts.

  See Task B.1.

- Define attrition resistance.

  The experiments suggested by Niro, Atomzier using silica as a binder did not produce the desired crush strength for Si supported catalysts.

A.2. Prepare Catalysts that can be Used to Determine the Role of Promoters for Low- and High-Alpha Catalysts

- Define Optimum SiO_2

  No scheduled or further activity to report.

- Define Optimum Al_2O_3

  No scheduled or further activity to report.

A.3. Prepare Catalysts that can be Used to Quantify the Role of K on Product Selectivity for both High- and Low-Alpha Catalysts

The work with low-alpha catalysts has been completed.

A.4. Complete the Optimization of Two Best Low-Alpha, Iron-Based Catalysts Developed During the Previous Contract

Completed.

A.5. Schedule of Activities for Next Quarter

- Continue experiments to develop a Si supported catalysts with sufficient robustness.

- Continue to develop a method to determine the robustness of Fischer-Tropsch catalysts.

B.0. - Task 2.0. Definition of Preferred Pretreatment for Both Low- and High-Alpha Catalysts

The goals of this task are to define the preferred treatment, to define the role of Cu and K during the pretreatment on activity and selectivity and to define the chemical and physical changes which occur during the preferred pretreatment. The subtasks address each of these goals.

B.1. Role of Cu in the Activation of Precipitated Low- and High-Alpha, Iron Based Fischer-Tropsch Catalysts

We have developed a precipitated FT catalyst with an atomic composition relative to iron of 100Fe/4.4Si/1.0K that shows high activity and remarkable stability. With the proper pretreatment, this catalyst has an initial carbon monoxide conversion greater than 90% and deactivates at a rate of 0.6% per week when operating at 270°C, 1.3 MPa, and a space velocity of 3.1 NL h^{-1} g(Fe)$^{-1}$. Activation with carbon monoxide (0.10 or 1.3 MPa) or syngas (H$_2$:CO=0.7, 0.10 MPa) at 270°C gives the highest activity. Activations with hydrogen are only successful when the catalyst is promoted with copper (Figure 1). In general, we have found that the catalyst activated with carbon monoxide had higher wax selectivity than when activated with syngas or hydrogen; however, all runs using the 100Fe/4.4Si/1.0K catalyst at 270°C resulted in a product distribution optimized for gasoline and light gases, not wax and oxygenates.

To decrease methane and increase wax selectivity, FTS temperature was decreased to 230°C. The highest activity at 230°C for a precipitated iron catalyst containing four atomic percent silicon was obtained with a potassium loading of

approximately five atomic percent (Figure 2). This was fortuitous, because the high potassium content also increased olefin yields; nevertheless, the activity of a 100Fe/4.4Si/5.2K catalyst was unacceptably low at the decreased temperature. Product selectivity was shifted toward the production of wax and α-olefins; however, carbon monoxide conversions were very low (Figure 3).

Results have shown that promotion with copper greatly improves catalyst performance at 230°C for catalysts pretreated with carbon monoxide, hydrogen or syngas (Figure 3). Promising findings have been obtained for a 100Fe/4.4Si/2.6Cu/5.2K catalyst. Activation with syngas (H_2:CO=0.7) has been found to result in a more active catalyst than pretreatment with carbon monoxide or hydrogen when operating at low temperature (Figure 3). Syngas activation resulted in a carbon monoxide conversion greater than 65% at 230°C, 1.3 MPa, and space velocity (H_2:CO=0.7) of 3.1 NL h^{-1} $g(Fe)^{-1}$. Methane selectivity below 2.5 weight percent and $C_{12}+$ selectivity greater than 70% have been achieved. Total olefin selectivity for the C_2-C_{11} fraction was greater than 75% and was predominantly α-olefins (Table 1).

Additional FTS runs are being made to optimize copper promotion and to determine how it affects FT activity. Early indications are that copper does increase the rate of reduction of iron oxide in hydrogen to the zero valent state. As an example, activation of a 100Fe/3.6Si/0.71K catalyst with syngas at high pressure resulted in poor activity. Addition of copper to the catalyst resulted in a substantial increase in the carbon monoxide conversion from less than 15% to greater than 50%. X-ray diffraction and Mössbauer spectroscopy analyses show that without copper the catalyst was 100% Fe_3O_4; however, with copper the catalyst was composed of a

mixture or Fe_3O_4 and iron carbides that are essential for high FT activity. Additional characterization is being conducted to determine the impact of copper on hydrogen and carbon monoxide treated catalysts.

B.2. Determine the Effect of K Content on Activation Procedures and Determinate if the Method of Addition has any Effect on Catalyst Activity and Life.

The work on the method of addition has been completed.

B.3. Physical and Chemical Changes that Occur During Pretreatment and Use

The TEM data from the University of New Mexico has not been received for the additional samples that were sent to them.

B.4. Effect of Carbon Deposition

No scheduled or further activity to report.

B.5. Schedule of Activities for Next Quarter

- Continue to determine the role of Cu for high-alpha catalysts.

- Continue to determine the effectiveness of Ba and Zn as promoters.

C.0. - Task 3.0. Catalyst Structure and Characterization

The goal of this task is to provide basic analyses (surface area, XRD) of all catalyst prepared and to provide additional techniques as required (Mössbauer, SEM, XPS, etc.) to answer specific questions or to provide basic required characterization data for the catalysts.

C.1. Schedule of Activities for Next Quarter

- Continue to provide the characterization data as required.

D.0. - Task 4.0. Catalyst Testing

The goals of this task are to operate the eight CSTR reactors, measure catalyst performance, determine the stable phases that exist during synthesis at low and high conversions and to determine the rates of interconversion of iron oxide and carbide.

D.1. Verify the Quality of Data Obtained from the CSTRs.

This task is now successfully completed.

D.2. Measure Catalyst Performance

The mechanism of the Fischer-Tropsch Synthesis (FTS) has elicited an ongoing debate since its discovery in the 1920s. Initially it was viewed that a bulk carbide formed and this was hydrogenated to produce hydrocarbons. During the 1950s the oxygenate intermediate received wide acceptance, primarily due to the ^{14}C tracer studies of Emmett and his coworkers. Subsequently, the results from surface science studies led to the revival of the carbide intermediate, but one that involved only the formation of a surface carbide.

The synthesis of methanol from syngas should provide a simpler mechanism that the FTS and, at the same time, provide some insight into the FTS mechanism. However, even the mechanism for the methanol synthesis is complex and involves controversy. Klier and co-workers (*Advan. Catal.*, **31**, 243 (1982)) advanced the view that methanol is synthesized from the CO component of the reactant mixture and that CO_2 served to maintain the catalyst in a partially oxidized state. On the other hand, it has been claimed that methanol is formed directly from CO_2 and not from CO. It appears that the contribution of CO and CO_2 to the synthesis of methanol depends upon the process conditions, and especially the partial pressures. While there are many differences between the FTS and methanol synthesis, they do have the

commonality of having both CO and CO_2 present in either the reactant feed or during the synthesis due to the activity of the iron-based catalysts for the water-gas-shift (WGS) reaction. The present work was initiated as an effort to assess the contribution of the WGS to the Fischer-Tropsch reaction since it was conceivable that CO_2 could be formed by another mechanism as shown below:

$$CO \rightarrow C_{ads} + O_{ads} \qquad\qquad 1)$$

$$O_{ads} + CO_{ads\ or\ gas} \rightarrow CO_2 \qquad\qquad 2)$$

Thus, the products from a combination of reactions [1] and [2] would be the same as if the WGS had operated. On the other hand, if the WGS reaction was rapid compared to the FTS we would expect ^{14}C, added in the CO_2, to rapidly redistribute and to be present in the CO. Surprisingly, when this experiment was performed, we found that the radioisotope distribution was such that it indicated that chain initiation could occur from an intermediate derived from CO_2 but that chain growth occurred using carbon derived only from CO. Furthermore, of the CO_2 that was converted, half, or more than half, was converted to hydrocarbons.

The run was conducted in a 1-liter CSTR system using a catalyst containing (based on Fe = 100) 4.4 Si and 0.71 K. The catalyst was pretreated with syngas (H_2/CO = 0.7) for 24 hr. at 270°C and 1 atm absolute. The synthesis was effected at 175 psig and 270°C with the molar gas compositions (H_2/CO/CO_2) and flows as follow: 0 to 480 hr. (50/25/25), 3.4 NL/hr-g.Fe; 504 to 720 hr. (66/0/34), 2.54 NL/hr-g.Fe; 744 to 1200 hr. (60/10/30), 2.83 NL/hr-g.Fe. Starting at hour 1,032 and continuing for 72 hr., $^{14}CO_2$ was added as a component of the feed gas. The $^{14}CO_2$ was added with the unlabeled CO (0.22 mole% $^{14}CO_2$). The hydrogen, CO and CO_2

streams feed to a mixing tank where the gases could be completely mixed prior to entering the CSTR.

The conversion data during the run are illustrated in Figure 4. During the period when equal molar amounts of CO and CO_2 were added (0 to 480 hr.), a portion of the CO was converted to CO_2 and the CO_2 conversion therefore appears to be negative. During the period when only H_2 and CO_2 were fed (504 to 720 hr.), the CO_2 conversion was about 25%. The conversion of CO_2 decreased when the amount of CO was increased during the third period of the run and, as expected, the lower partial pressure of CO led to a lower percentage conversion of CO.

During the period of $^{14}CO_2$ addition the conversion of H_2 was about 32%, of CO about 74% and of CO_2 about 9%. During this period CO_2 was converted to CO so that the gases exiting the reactor had essentially the same radioactivity/mole (1.7×10^2 for CO and 1.3×10^2 for CO_2). Thus there was certainly interchange between these two compounds toward a similar specific label.

The analysis of the C_4-C_{10} hydrocarbons indicate that all hydrocarbons have radioactivity/mole (Figure 5). This is a not a surprising result . A similar result was obtained when the $^{14}CO_2$ was added as a tracer but at a low chemical composition (0.2 mole% of the CO). The result that was obtained with low concentration of CO_2 is the one expected when the $^{14}CO_2$ serves to initiate but that the chain growth is due to the unlabeled CO.

If there was significant WGS conversions and it occurred at a rate that was similar to or exceeded that of the hydrocarbon synthesis one would expect the CO to contain significant ^{14}C as well as the CO_2. If the CO and CO_2 served initiate and the CO to cause chain growth, the radioactivity/mole should increase with carbon number

and the slope of the line should be equal to the ^{14}C content of the CO. Thus, if the WGS reaction had attained equilibrium prior to the beginning of the FTS, the radioactivity of C^1 should be that of the CO_2 (the same as CO) that initiates the reaction and the slope of the line defining the radioactivity/mole versus the carbon number should have had a slope defined by the radioactivity of the CO. This is exactly the result that is obtained for the hydrocarbons in the carbon number range C_1 to C_4 but the trend does not apply for carbon numbers higher than 4.

One of the puzzling features of the earlier tracer studies was the result that the low isotopic distribution for the lower carbon number compounds was consistent with chain initiation by either an added alcohol or alkene; however, the C^{14}/mole for the higher carbon number compounds decreased with increasing carbon number (Figure 6). The slope of the line for the higher carbon number compounds for many runs was in the range of -0.06 to -0.24 and appeared to depend upon the operating conditions. Originally the reason advanced for the decrease in the radioactivity/mole for the higher hydrocarbons was that two independent FTS chains contributed to the mechanism. However, more recent work indicates that the accumulation of hydrocarbons may also impact the ASF plot and even give the appearance of a two-alpha mechanism.

The slope of the line, based on the log as was done in Figure 6, is -0.06, in reasonable agreement with the lower values obtained earlier. Thus, it appears that the accumulation of hydrocarbons in the CSTR prior to the addition of the $^{14}CO_2$ dilutes the products in the C_4-C_9 hydrocarbon range sufficiently to cause the apparent decline in the radioactivity.

The present data together with our earlier data are consistent with the high partial pressure of CO inhibiting the adsorption of CO_2 and this, combined with the

low H_2/CO ratio, caused CO_2 to only initiate chain growth. However, the lower CO partial pressure in the present study together with the higher H_2/CO ratio caused significant WGS to occur. Thus, the synthesis was conducted with the added ^{14}C about equally distributed between the CO and the CO_2, and this caused a linear increase in the radioactivity/mole for the C_1-C_4 hydrocarbons, as seen in Figure 5. The accumulation of unlabeled hydrocarbons causes the radioactivity to be diluted for the higher carbon number hydrocarbons and the actual decline in the radioactivity/mole versus carbon number plot.

D.3. Determine Stable Phases that Exist During Synthesis at High and Low CO Conversion Levels

The CHO system is of great importance in many areas of modern technology such as combustion, gasification, fuel cell and the Fischer-Tropsch (F-T) synthesis process. The species most likely to be present in the greatest amounts are among those which are most stable under the conditions of interest, i.e., those having the lowest value of the free energy of formation. In a system containing the elements of carbon, hydrogen and oxygen in the temperature ranges of 298K to 1500K and a pressure of one atmosphere, the most stable species are carbon, carbon oxide, carbon dioxide, hydrogen, water and methane. Therefore, the system containing C_1 gases (CO, CO_2, H_2O, H_2 and CH_4) was selected in this study to perform a set of thermodynamic calculations. Furthermore, for F-T synthesis reaction, an iron catalyst is usually employed. On contacting with the pretreating and reacting gases, the iron can be formed as an iron carbide, which is a catalyst for F-T synthesis and/or an iron oxide, which is not desired for F-T synthesis. It is practical to see whether or not the gas phase composition lie in ranges where the iron carbide is thermodynamically

14

favored during the course of catalyst pretreatment and synthesis. Therefore, the systems containing $Fe/Fe_xC/gases$ equilibria and $Fe/Fe_xO_y/gases$ equilibria were also investigated in this study. A convenient and informative method for the presentation is to show the iron carbide or iron oxide formation boundaries for the ternary CHO system using a set of triangular coordinates. The generality of the phase diagram becomes clear when it is recognized that C:H:O ratios of the system completely determine whether or not carbon, iron oxide and/or iron carbide are formed for a given composition of gases.

This study considers the CHO gas phase compositions in equilibrium with iron and/or graphite (C) over different temperatures (200°C - 800°C) at a pressure of 15 atmospheres. Different forms of iron oxide, i.e., Fe_3O_4, Fe_2O_3 and FeO, and iron carbide, i.e., Fe_3C, $Fe_{2.2}C$ and Fe_2C, were observed during F-T synthesis. For simplicity, only Fe_3O_4 and Fe_3C were used for this calculation.

In the F-T synthesis over an iron catalyst, Fe_3C, Fe_3O_4, and C may be formed by reaction (1), (2), and (3) respectively

$$H_2 + CO + 3Fe = Fe_3C + H_2O \tag{1}$$

$$3Fe + 4H_2O = Fe_3O_4 + 4H_2 \tag{2}$$

$$2CO = C + CO_2 \tag{3}$$
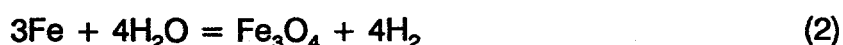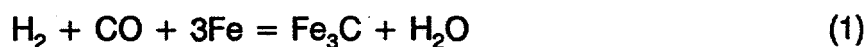
The gas components are subject to water-gas shift reaction

$$H_2O + CO = H_2 + CO_2 \tag{4}$$

and methane may be included as follows:

$$C + 2H_2 = CH_4. \tag{5}$$

Also, the HC components may be formed as, for example

$$CO + H_2 = CH_2 + H_2O \tag{6}$$

15

$$nCH_2 = (CH_2)_n. \qquad (7)$$

Three pertinent equilibria, C/gases, Fe/Fe$_3$O$_4$/gases and Fe/Fe$_3$C/gases were calculated by modifying the method presented by Cairns and Tevebaugh (*J. Chem. & Eng. DATA*, **9**, 453 (1964)). Figures 7 to 10 are phase diagrams showing the four regions defined by the equilibria defined by the reactions of Fe/Fe$_3$O$_4$/gases (upper line), Fe/Fe$_3$C/gases (middle line) and C/gases (bottom line) at a pressure of 15 atmospheres and temperatures of 300, 527, 200 and 250°C, respectively. These lines calculated for the reactions indicated divide the gas composition space into four regions designated A, B, C and D. In region A, the iron catalyst in contact with gas of the composition defined for region A will be present only as Fe$_3$O$_4$ and no free caron will be present. In region B the iron will still be present at Fe$_3$O$_4$ but in addition to Fe$_3$O$_4$, solid carbon (graphite in this example) will also be present. In region C, three solids will be present: Fe$_3$O$_4$, Fe$_3$C and carbon. In region D, Fe$_3$O$_4$ will not be present; thus, as the gas composition is altered to fall in region D, both Fe$_3$C and C will be present at equilibrium. From these diagrams, one can delineate regions where Fe$_3$C, Fe$_3$O$_4$ and/or C would be expected to be present for different gas mixtures composed hydrogen, oxygen and carbon at different temperatures. For example, for a gas mixture represented by a position which is located in region D, Fe$_3$C is the solid iron phase that is thermodynamically favored. A tie line for the composition of the syngas for F-T synthesis that we use (H$_2$/CO = 0.7) and with different H$_2$/CO mole ratios representing various conversion levels is also included in Figure 7. This tie line clearly shows that in order to obtain 100% of Fe$_3$C, the H$_2$/CO mole ratio of the syngas must be less than 0.75.

One may assume that 100% of Fe_3C is obtained after pretreating with the syngas which compositions fall in the region that Fe_3C is thermodynamically favored. During the course of F-T synthesis, gas compositions may change and cause a catalyst phase to change from Fe_3C to Fe_3O_4. Previous studies showed that the formation of H_2O during the F-T synthesis, i.e., reaction 6, is the major reason that Fe_3C will change phase to Fe_3O_4. In order to simulate this phase change, reactions 1, 2, 4, and 6 were applied. The initial reactions of F-T synthesis may be described as

$$H_2O + CO \longrightarrow H_2 + CO_2 \qquad (4)$$

$$CO + H_2 \longrightarrow CH_2 + H_2O. \qquad (6)$$
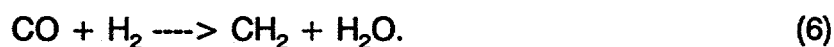
Under each particular feedstock ratio of H_2/CO, the composition of all gases can be calculated by using material balance equations if the conversions of CO and H_2 are known. Initially, it was assumed that 100% of Fe_3C was placed in a "flexible reactor" whose volume can increase with an increase of gases fed but still maintain a constant pressure, i.e. 15 atm. The same composition of gases were then continuously charged into this reactor at a constant flow rate. Some gases may react with Fe_3C to covert it to Fe_3O_4 until the equilibrium was reached. This equilibrium reaction can be described as

$$Fe_3C + 4H_2O = Fe_3O_4 + 2H_2 + CH_4. \qquad (1)+(2)$$
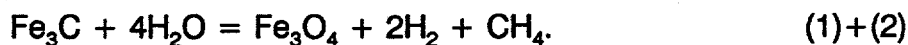
By doing this, one can predict the time needed to convert all Fe_3C to Fe_3O_4 at a particular reaction condition. For a typical F-T synthesis (catalyst = 15 g of Fe, T = 300°C, P = 15 atm, H_2/CO = 0.67 at a flow rate of 3.1 NL/hr./g of Fe, and an alpha value = 0.7), conversions of H_2 and CO are approximately 0.9 and 0.86, respectively. Under these reaction conditions, the percentage of the change of Fe_3C to Fe_3O_4 with time and total amount of gases remaining in the reactor with time can be seen in

Figures 11 and 12, respectively. From Figure 11, one can see that it takes approximately 3.7 hours to completely convert Fe_3C to Fe_3O_4 if the reactions are rapid enough to establish the equilibrium state at all times. Figures 13 and 14 show that the volume needed to completely converts Fe_3C to Fe_3O_4 is approximately 15 liters (at 15 atm. and 300°C) or 120 NL (at 1 atm. and 25°C), respectively.

CHO phase diagram is a simple way to allow one to precondition the catalyst surface (i.e., Fe_3C) and then feed a gas mixture that favors only the preconditioned surface phase. Also, the surface phase change, if any, can be monitored *in situ* by knowing the gas composition in the reactor.

Comparison with Experimental Data

A series of F-T synthesis runs using a slurry reactor were employed. The molar ratio of the syngas feed ($H_2/CO=0.67$), pressure (175 psi), and temperature (270°C) were held constant while flow rates of syngas were varied between 9.5 to 75.6 NL/hr. for CO and 6.4 to 50.6 NL/hr. for H_2. The composition of the gas phase for each run is reported in Table 2. Hydrocarbons formed (i.e., C_1 to C_{35}) during reaction were reported in this table as an average value of $C_x H_y$. The mean carbon number (x) of the hydrocarbon products is given by

$$x = 1/ (1 - \alpha) \tag{8}$$

where α refers to chain growth probability. Since the α value for these particular runs is equal to 0.75, the mean carbon number x can be obtained, which is equal to 4. The mean hydrogen number in the products then can be calculated as

$$y = \{\Sigma[H/C]_i \cdot N_i / \Sigma N_i \} * x \tag{9}$$

where the mean carbon number x = 4, i denotes a hydrocarbon with carbon number equal to i, and N denotes the molar fraction of each hydrocarbon. Figure 15 indicates

that at higher conversion, i.e., X_{CO} = 0.69 to 0.86, the solid iron phase

thermodynamically favored is Fe_3C. However, at lower conversion, i.e., X_{CO} = 0.23 to

0.46, both Fe_3C and Fe_3O_4 are thermodynamically favored. Table 2 shows that the

concentration of H_2O and CO decreased with the increased conversion of CO.

However, the concentration of CO_2 increases with CO conversion. Therefore it may

be suggested that H_2O and CO play a more important role than CO_2 to oxidize Fe_3C

to Fe_3O_4. Figure 16 indicates that conversion of CO and H_2 are approximately

identical, i.e., X_{CO} = X_{H2} = 0.69, at total flow rate (CO+H_2) equal to 31.3 NL/hr. One

may called this particular flow rate as a critical flow rate. At a flow rate lower than the

critical rate, conversion of CO is greater than that of H_2. However, the conversion of

H_2 is greater than that of CO at a flow rate faster than the critical rate. This is due to

the effect of water-gas-shift (WGS) reaction since the WGS reaction will consume more

CO and generate H_2. At lower flow rates the WGS reaction becomes more significant

than at higher flow rates. Therefore the WGS reaction is an important side reaction for

the F-T synthesis. Furthermore, since the WGS reaction can consume H_2O, which is

produced during F-T synthesis and is a major compound to oxide Fe_3C to Fe_3O_4, the

importance of the critical flow rate can then be explained using phase diagram (Figure

15). It is clear to see from Figure 15, for the flow rate slower than the critical rate, the

iron phase thermodynamically favored is Fe_3C. However, for the flow rate faster than

the critical rate, both Fe_3C and Fe_3O_4 are thermodynamically favored. Again this can

be explained as the effect of WGS in F-T synthesis. It is important to note that the

data point that represent the gas compositions at critical flow rate is identical to the

point that represents the feed composition, i.e., H_2/CO=0.67, in the phase diagram.

These results indicate that the phase diagram with gas phase composition data can